NeuroImage 62 (2012) 699–705

Contents lists available at SciVerse ScienceDirect

NeuroImage

journal homepage: www.elsevier.com/locate/ynimg

Review

Ultrafast inverse imaging techniques for fMRI

Fa-Hsuan Lin [a,b,c], Kevin W.K. Tsai [a], Ying-Hua Chu [a], Thomas Witzel [b], Aapo Nummenmaa [b,c], Tommi Raij [b], Jyrki Ahveninen [b], Wen-Jui Kuo [d,*], John W. Belliveau [b]

[a] Institute of Biomedical Engineering, National Taiwan University, Taipei, Taiwan
[b] MGH-HST Athinoula A. Martinos Center for Biomedical Imaging, Charlestown, MA, USA
[c] Department of Biomedical Engineering and Computational Science, Aalto University School of Science and Technology, Espoo, Finland
[d] Institute of Neuroscience, National Yang Ming University, Taipei, Taiwan

ARTICLE INFO

Article history:
Accepted 10 January 2012
Available online 21 January 2012

Keywords:
InI
Fast imaging
Parallel imaging
Inverse problem

ABSTRACT

Inverse imaging (InI) supercharges the sampling rate of traditional functional MRI 10–100 fold at a cost of a moderate reduction in spatial resolution. The technique is inspired by similarities between multi-sensor magnetoencephalography (MEG) and highly parallel radio-frequency (RF) MRI detector arrays. Using presently available 32-channel head coils at 3T, InI can be sampled at 10 Hz and provides about 5-mm cortical spatial resolution with whole-brain coverage. Here we discuss the present applications of InI, as well as potential future challenges and opportunities in further improving its spatiotemporal resolution and sensitivity. InI may become a helpful tool for clinicians and neuroscientists for revealing the complex dynamics of brain functions during task-related and resting states.

Contents

Introduction

Functional MRI (fMRI) in humans (Belliveau et al., 1991) using the blood-oxygen level dependent (BOLD) contrast (Kwong et al., 1992; Ogawa et al., 1990) allows non-invasive detection of hemodynamic responses associated with neural activity. Neuronal activity results in a complex series of hemodynamic changes in blood flow, volume, and oxygenation, the combination of which results in the BOLD signal (Logothetis et al., 2001). Single-shot echo-planar imaging (EPI), which has been the principal technology for fMRI, has a sampling rate of 1–3 s and spatial resolution of 3–5 mm for 3D brain imaging.

Because of the sluggishness of the hemodynamic response relative to the underlying rapid electrophysiological events, one might think that improving the sampling rate of fMRI might not reveal information about brain dynamics. However, fast sampling of fMRI, achieved by scanning only a single or a small number of EPI slices (resulting in very limited spatial coverage), has found differences in the BOLD onset times across different brain areas in the order of hundreds of milliseconds (Menon et al., 1998). Several studies have also used jittered stimulus timing to increase the effective sampling rate achieved during multislice EPI ((Friston, 2007; Rosen et al., 1998) for reviews) but such studies are complicated by that the required acquisition time increases linearly with the amount of slices and desired sampling rate, typically leading to impractical scan durations (~hours). BOLD fMRI has also allowed detection of interactions across neural systems at a millisecond time scale (Ogawa et al., 2000). Therefore, BOLD responses may convey more relevant and finely

* Corresponding author.
E-mail address: wjkuo@ym.edu.tw (W.-J. Kuo).

1053-8119/$ – see front matter © 2012 Elsevier Inc. All rights reserved.
doi:10.1016/j.neuroimage.2012.01.072

graded timing information than usually believed. For these purposes it is important to differentiate between BOLD *sampling rate* and its effective *interregional temporal resolution*. The former indicates how fast the planar or volumetric fMRI data can be acquired, which is the principal topic of the present review. The latter reflects the smallest significant interregional BOLD signal delays; here, interregional vascular and biochemical differences could potentially confound the ability of BOLD imaging to accurately reflect neuronal (electrophysiological) activation sequences across brain areas. Obviously, fast BOLD sampling techniques would greatly facilitate investigating the merits and limits of the timing information embedded in BOLD signals. MRI has also been considered for detecting fast functional changes related directly to neuronal (electrophysiological) activity (Xiong et al., 2003) but efforts to identify suitable MRI contrast mechanisms have been hampered by the lack of image acquisition and reconstruction methods that could achieve the required very high sampling rate, which is another area where techniques developed for fast BOLD imaging might become useful.

The sampling rate of gradient-encoded MRI is limited by the time required to traverse k-space. While classical gradient- or spin-echo images complete one line in the k-space in each excitation, EPI and spiral imaging utilize fast switching gradients to traverse a 2D k-space in a single RF excitation (Blum et al., 1987; Mansfield, 1977), allowing the acquisition of a single slice image in ~80 ms with 3 mm isotropic resolution. Further improvements can be achieved by optimizing the k-space sampling and reconstruction methods, for example, by using partial k-space sampling (McGibney et al., 1993) or by methods based on *a priori* information (Tsao et al., 2001) such as key-hole imaging (Jones et al., 1993; van Vaals et al., 1993), singular-value-decomposition MRI (SVD-MRI) (Zientara et al., 1994), or wavelet encoded MRI (Panych et al., 1993; Weaver et al., 1992).

Recently, parallel MRI methods that reconstruct images using spatial information derived simultaneously from multichannel RF receiver coil arrays have dramatically improved the sampling rate of dynamic MRI. Reconstruction methods such as k-space SMASH (Sodickson and Manning, 1997), GRAPPA (Griswold et al., 2002), and image domain SENSE (Pruessmann et al., 1999) methods, all of which share a similar theoretical background (Sodickson and McKenzie, 2001), can accelerate the data acquisition rate by reduced k-space traversal at a cost of reduced signal-to-noise ratio (SNR). Additional benefits of parallel MRI include reduced gradient-switching noise (de Zwart et al., 2002), reduced geometrical distortion due to higher bandwidth in the phase-encoding direction compared to single-shot EPI (Schmidt et al., 2005; Weiger et al., 2002) or in diffusion weighted (Bammer et al., 2001) imaging, and superior cancellation of ghosting artifacts (Kellman and McVeigh, 2001). The acceleration rate of parallel MRI is limited by the phase-encoding schemes and by the available independent spatial information encoded in the array. Mathematically, the constraint manifests itself as a problem of solving an over-determined linear system. Increasing the number of channels can thus increase the acceleration rate in parallel MRI. The number of channels in head coil arrays has been increased from 8 to 16 (Bodurka et al., 2004; de Zwart et al., 2002, 2004), 23, 32, and 90 (Wiggins et al., 2005a, 2005b). Recently, a dedicated 64-channel linear planar array has been developed to achieve 64-fold acceleration (McDougall and Wright, 2005). Parallel imaging can also be combined with EPI (Golay et al., 2000; Preibisch et al., 2003; Schmidt et al., 2005; Weiger et al., 2002). Accelerated multi-slice EPI acquisitions based on simultaneous excitation, simultaneous echo refocusing, and signal separation using coil sensitivity profiles have been demonstrated at both 3T and 7T, offering maximal full-brain sampling resolutions of about 0.4 s (Feinberg et al., 2010; Larkman et al., 2001; Setsompop et al., 2012).

Inverse imaging (InI) (Lin et al., 2006) is based on the essential similarities (Hennig, 2005) between the geometric configurations of the 90-channel MRI head array (Wiggins et al., 2009) and those of whole-head MEG/EEG sensor systems (Hamalainen et al., 1993). The MEG sensors detect magnetic fields generated by neural currents (Hamalainen et al., 1993), whereas MRI detects oscillating electromagnetic fields from magnetization precession. While MEG derives all of its spatial information from the geometrical arrangement of the detectors, MRI still relies heavily on gradient encoding. Based on these analogies, we generalized the parallel MRI reconstruction technique to exceed the limitations of the over-determined linear system in parallel MRI. InI engages an under-determined linear system in order to reconstruct images using dramatically accelerated MR acquisition (Lin et al., 2006). This method is a generalization of prior-informed parallel MRI (Lin et al., 2004, 2005, 2007). Similar to the MR-encephalography (MREG) (Hennig et al., 2007), InI fMRI offers an improved sampling rate due to the minimal time required to traverse k-space. Rather than heavily relying on gradient encoding, InI derives spatial information by solving inverse problems using data simultaneously acquired from all channels in the array.

Currently, when using a standard 32-channel head coil array, InI allows 100 ms sampling rate with whole-brain coverage and about 5 mm spatial resolution at the cortex. Below, we will discuss applications of InI and opportunities for its further technical development.

Applications of InI

Compared to EPI, InI offers 1–2 orders of magnitude faster sampling rate at the cost of slightly reduced spatial resolution in one encoding direction. The acquisition speed can be exploited in different dynamic imaging applications. fMRI with a fast sampling rate may provide hemodynamic timing information at neuronally relevant scales (Lin et al., 2010a). InI can also be used to monitor and to suppress physiological fluctuations in order to improve the sensitivity of detecting BOLD activity (Kruger and Glover, 2001; Lin et al., in press). This is due to the fact that the conventional 0.5 Hz/volume sampling rate is too low to resolve the aliased cardiac (1.0–1.3 Hz) and respiratory (0.2–0.3 Hz) cycles. Additionally, fMRI with a faster sampling rate could potentially improve the power of detecting causal modulations among brain areas (Deshpande et al., 2010; Kayser et al., 2009; Roebroeck et al., 2005).

BOLD responses are about 10–30 s long and temporally smooth. However, they may also surprisingly accurately reflect neuronal timing (see Introduction). Furthermore, event-related fMRI (Dale and Buckner, 1997; Rosen et al., 1998) studies have suggested that the durations of the BOLD response in motor planning areas correlate with behavioral reaction times (Menon et al., 1998; Richter et al., 2000), and that relative delays between visual hemifield stimuli correlate with inter-hemispheric BOLD latency differences (Huettel and McCarthy, 2000; Menon et al., 1998). Timing differences across brain areas have also been reported in previous event-related BOLD chronometry studies ((Kim and Ogawa, 2002; Rosen et al., 1998) for reviews). Using a two-choice reaction time visuomotor task and InI measurements, our preliminary results suggest that InI may resolve even small temporal delays between cortical areas at group level (Lin et al., 2010a). Independently, it is possible to use InI to investigate the trial-by-trial variation in EEG and hemodynamics (LeVan et al., 2011).

InI may be used to monitor and suppress physiological noise in BOLD fMRI experiments (Lin et al., in press). Physiological noise is generally proportional to the signal, and going to higher field strength increases its contribution to overall variance (Kruger and Glover, 2001). In addition, at a given field strength, improvements to receiver hardware and signal reception (Bodurka et al., 2007) can result in physiological noise dominating the variance in fMRI time-course data. It has been reported that cardiac and respiratory noise account for approximately 33% of the total physiological noise encountered in human gray matter in 3T fMRI studies (Birn et al., 2006; Kruger and Glover, 2001). In attempts to mitigate the effects of physiological

noise in fMRI experiments via digital filtering (Biswal et al., 1996) or signal processing (Glover et al., 2000; Hu and Kim, 1994), there are two competing factors: the image volume sampling rate and spatial coverage. Currently, echo-planar imaging (EPI) requires approximately 2–4 s to acquire a full brain volume. EPI therefore lacks sufficient speed to avoid aliasing of higher frequency periodic cardiac and respiratory effects. InI allows the use of straightforward digital processing methods for suppressing physiological noise sources without the need for external physiological monitoring devices. Compared to spatially smoothed EPI data, filtered InI data has a 58% higher peak z-value (Lin et al., in press). This result is higher than the 4% increase observed when using adaptive filtering, which has comparable performance to that seen with the RETROICOR method (Deckers et al., 2006). This demonstrated InI's advantages of suppressing physiological noise in fMRI experiments.

In multi-slice EPI, different slices are acquired sequentially at different times. Slice timing correction is typically done by incorporating the convolution between the canonical hemodynamic response function and its temporal derivative to stimulus onsets as regressors in the design matrix of the General Linear Model (Friston et al., 1998). InI is a single-shot 3D imaging method and thus does not suffer from errors resulting from timing differences across slices and attempts to correct for them.

InI can also improve the sensitivity to BOLD contrast by using multi-echo acquisitions (Poser and Norris, 2009; Posse et al., 1999). For example, within 2 s (the TR typical in multi-slice EPI), InI allows 8 echoes with two averages to improve the sensitivity of detecting hemodynamic responses. In this case some spatial resolution is traded off for acquiring data with different TEs optimized for different parts of the brain.

Coupling systems and synchronization phenomena in brain have been widely investigated (for review, see (Singer, 1999)). Functional connectivity (Friston et al., 1993) studies the temporal coherence among brain areas. For example, distributed cortical, sub-cortical, and cerebellar areas are jointly modulated by the rate of motor responses (Lin et al., 2009). At rest, multiple areas in the "default-mode" network also have highly correlated spontaneous hemodynamics (Raichle et al., 2001) and electrophysiological activities (Mantini et al., 2007). Such functional connectivity has been usually analyzed by studying the correlation and covariance of the time series between different brain areas. InI could help such functional connectivity studies in many ways. First, present functional connectivity studies, due to the slow sampling of EPI, can only detect very slow (<0.1 Hz) fluctuations in the network, whereas the brain apparently also demonstrates functional connectivity at much higher frequencies (Lee et al., 2011). The high sampling rate of InI can be used to explore the different spectral contributions to the functional connectivity networks. Further, in distinguishing between direct and indirect modulations between brain areas using, for example, partial correlation analysis, the number of degrees of freedom (df) in the time series is critically important (Smith et al., 2011). However, traditional EPI usually lacks a sufficient df when the model includes a realistically large number of areas and their connections. InI can mitigate this challenge by providing a large amount of data, although it has to be noted that the samples are temporally correlated and appropriate corrections are needed to ensure that the modeled data are sufficiently uncorrelated.

Different from functional connectivity analysis, *effective connectivity* analysis (Cabeza et al., 1997; Friston, 2007; Friston et al., 1997) attempts to reveal causal influences among active brain areas. Different from Structural Equation Modeling (Lin et al., 2009; McIntosh and Gonzalez-Lima, 1994) or Dynamic Causal Modeling (Friston et al., 2003), Granger causality (GC) is a data-based approach for estimating directional interactions without first specifying the existence of directed interactions in a network. Using fMRI time series, GC estimates causal modulations by checking whether the residual errors of a modeled time series is statistically smaller after giving another time series. Since causal relations are derived from fMRI time series, both GC (Deshpande et al., 2010; Kayser et al., 2009; Roebroeck et al., 2005) and Dynamic Causal Modeling (Kasess et al., 2010) favor acquisitions at high sampling rate in order to reveal more accurate causal modulations when regional vascular response variability is appropriately accounted for. Our preliminary studies demonstrate how InI can be used to improve the sensitivity of detecting causal modulation using BOLD-contrast fMRI data. Specifically, InI with TR = 100 ms detects clear feed-forward modulations in a visuomotor two-choice reaction time task (Chu et al., 2011; Lin et al., 2011).

Lastly, spatial localization using highly parallel RF detection may also be applied to reduce the acoustic noise in MRI. MRI acoustic noise is generated by the induced Lorentz force as the passing current on the gradient coil perpendicular to the main field. The Lorentz force acting on the gradient coil causes vibration similar to a loudspeaker (Schmitt et al., 1998). This acoustic noise is particularly prominent in EPI, where fast oscillatory gradients are used to accelerate k-space traversal. It has been shown that EPI gradient switching itself can elicit auditory BOLD-contrast responses (Bandettini et al., 1998). It has also been suggested that acoustic noise can result in modulation of visual areas (Raij et al., 2010; Zhang et al., 2005). Thus, in the presence of acoustic scanner noise, EPI fMRI studies of the visual and auditory systems can be difficult to interpret. To mitigate this difficulty, sparse sampling methods have been utilized (Edmister et al., 1999; Hall et al., 1999; Schwarzbauer et al., 2006; Talavage et al., 1999). Alternative approaches have utilized smoothing of gradient waveforms to suppress the acoustic noise level (Hennel et al., 1999). However, with this technique, the soft sinusoidal gradient pulses limit the total gradient moment and thus decrease the spatiotemporal resolution. Using a minimal number of smooth gradient pulses, InI may still provide a reasonable spatiotemporal resolution with much quieter sound levels.

Technical challenges and future opportunities

Spatial resolution

The current implementation of volumetric InI uses 100 ms sampling rate for whole-brain coverage. This speed is accompanied with a moderate loss of spatial resolution (in the InI encoding direction only). Since InI solves underdetermined linear systems during image reconstructions, the spatial resolution of reconstructed InI data depends on the choice of the reconstruction methods. In general the spatial resolution is lower at the center of the brain and higher at the cortex (Lin et al., 2008a, 2008b, 2010b; Liou et al., 2011). Quantitatively, the spatial resolution is around 5 mm at cortex and 20 mm at the center of the brain when the minimum-norm estimate is used (Lin et al., 2008a). This compromise seems acceptable since most EPI analyses spatially smooth the data using a volumetric kernel with 6–12 mm full-width-half-maximum. There are two approaches to reduce the loss of spatial resolution. First, reconstructions algorithms can be modified since there exist an infinite number of solutions in ill-posed underdetermined linear systems. Second, InI acquisitions can be modified. These approaches are discussed below.

For computational efficiency and solution stability, InI reconstruction utilizes the minimum-norm estimate (MNE) (Lin et al., 2008a). The mathematical constraint of minimizing the L2 norm of the unknown prefers spatially diffuse solutions. Replacing the minimizing L2 norm constraint by minimizing L-p norm constraint ($p<2$) can reduce spatial blurring (Tarantola, 2005). With $p=1$, the solution has been shown to be spatially focal in MEG and EEG source modeling (Chang et al., 2010; Matsuura and Okabe, 1995; Uutela et al., 1999). InI may improve the spatial resolution by employing the same mathematical constraint at the cost of computational complexity using the Linear Programming or convex optimization.

Other than minimizing the norm of the solution, InI can be reconstructed using spatial filtering (Lin et al., 2008b; Liou et al., 2011) and

k-space data interpolation (Lin et al., 2010b). Beamformers create separate spatial filters at each source location to minimize the output variance (Lin et al., 2008b) or amplitude (Liou et al., 2011) for a higher sensitivity in detecting dynamic changes. However, spatial filtering cannot estimate solutions satisfying the forward problem. Thus, instantaneous reconstructions will be quite different from the reference scan. Similar to the GRAPPA formulism (Griswold et al., 2002), K-space InI reconstruction exploits the dependency between data in neighboring k-space locations from different channels of the coil array to reconstruct highly under-sampled data (Lin et al., 2010b). The K-InI reconstruction offers a compromise in computational efficiency, detection sensitivity, and quality of instantaneous image between MNE and spatial filter reconstructions.

Among different InI reconstruction methods, the MNE is the most computationally efficient, because of the availability of a closed form solution (Lin et al., 2006a, 2008a). However, a spatial filtering technique minimizing the output variance provides higher detection sensitivity to brain activation and higher spatial resolution than MNE (Lin et al., 2008b). At the cost of computational efficiency, the detection sensitivity of the LCMV spatial filtering can be further improved by using a constraint to minimize the output amplitude (Liou et al., 2011). At the same time, the spatial filter techniques cannot reconstruct images with similar anatomical features and contrast as the reference scan. K-InI reconstruction provides a trade-off between MNE and spatial filtering methods in terms of computational efficiency, spatial resolution, and detection sensitivity (Lin et al., 2010b).

InI spatial resolution can also be improved by modifying acquisitions. In most BOLD-contrast fMRI experiments, repetitive measurements are usually required to compensate the relatively low contrast-to-noise ratio (CNR) in order to detect activated brain areas with a sufficient statistical significance. Such a data acquisition protocol opens up the possibility of combining InI acquisitions to improve spatial resolution. For example, COBRA combines different in-plane projection data to achieve highly accelerated 2D fMRI (Grotz et al., 2009). It is also possible to combine orthogonal projections in 3D to further improve the spatial resolution of volumetric acquisitions (Tsai et al., 2011). Fig. 1 shows that when three orthogonal projection images were combined, BOLD signal has higher spatial resolution in the visual and motor

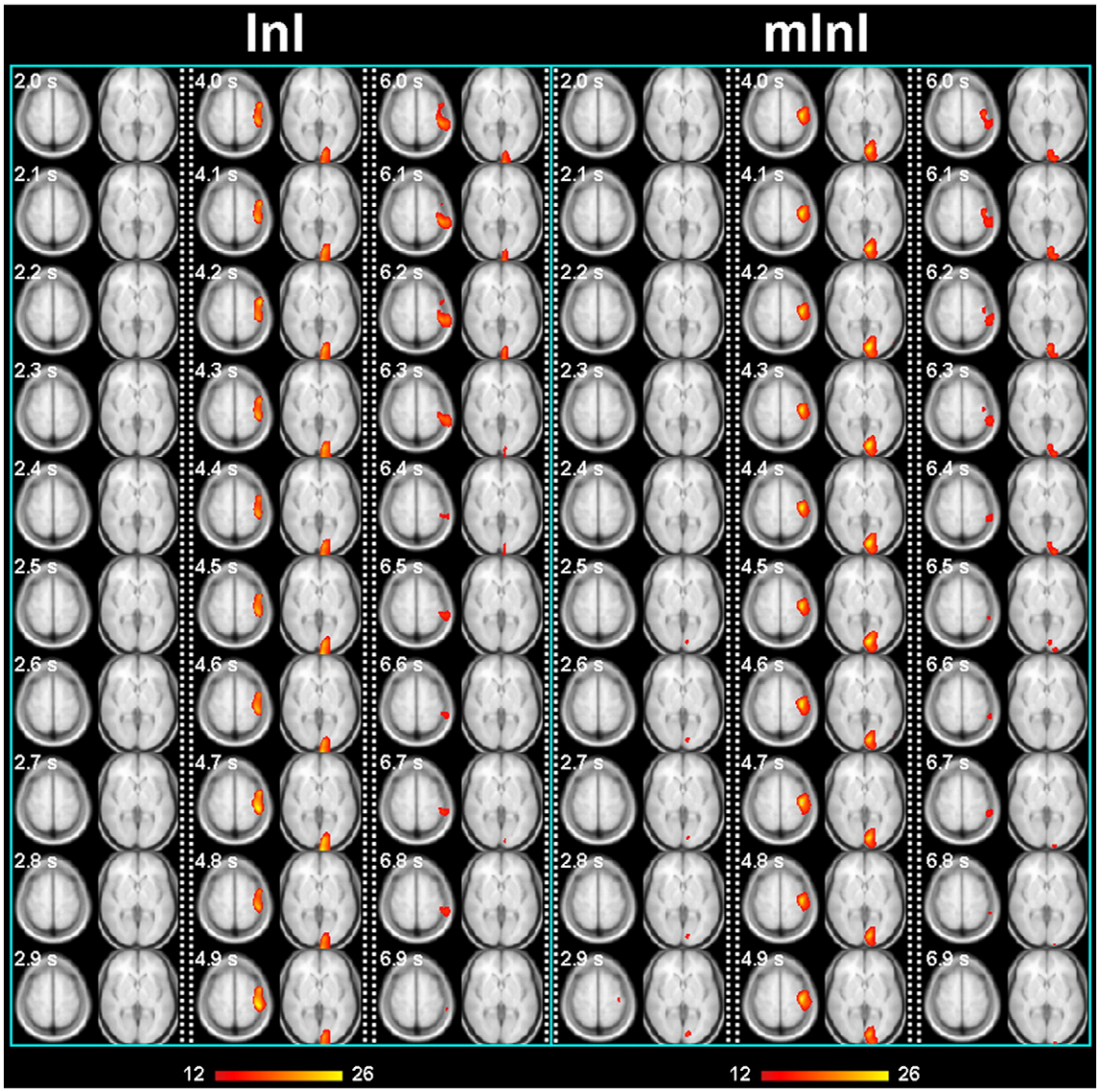

Fig. 1. Spatiotemporal activity of the visual and motor cortices in BOLD-contrast fMRI using two different InI versions. Left. The anterior-posterior direction was encoded with InI and the other two directions with standard EPI methods (frequency and phase). Right. Multi-projection InI (mInI) composed of three InI runs where the InI encoding direction was either anterior–posterior, left-right, or superior–inferior. mInI shows improved spatial resolution due to less spread along the anterior–posterior direction than InI. Note that the time axis is not continuous; instead, three separate time windows of interest are displayed at 100 ms steps (2–3 s, 4–5 s, and 6–7 s).

cortices (less blurring along anterior–posterior direction than InI using only one coronal projection) in a two-choice reaction time task.

InI and COBRA use a (rotated) rectilinear k-space trajectory. When leaving out phase encoding, we obtain projection data and the spatial resolution becomes rather anisotropic. Other sophisticated trajectories, such as the single-shot Rosette trajectory (Zahneisen et al., 2011a), may improve the homogeneity of the spatial resolution. Recently, multiple concentric-shell trajectory has also been realized to improve the spatial resolution of fast fMRI (Zahneisen et al., 2011b). MREG using a Rosette or a concentric-shell trajectory is less sensitive to susceptibility artifacts, potentially due to over-sampling around the center of the *k*-space. Yet these acquisitions come at the price of trajectory calibration and reconstructions complexity.

Improving the RF and gradient hardware can also increase InI spatial resolution. Our present 3D InI experiments have used a 32-channel head coil arrays with elements evenly distributed like a soccer ball. Without reaching the electromagnetic theory limit (Ohliger et al., 2003; Wiesinger et al., 2004), further increasing the channels of a head array, such as in a 96 channel head coil array (Wiggins et al., 2009), can increase the amount of non-redundant spatial information among RF channels. This can be used to improve the spatial resolution of InI.

InI can be closely related to the echo-volume imaging (EVI) (Mansfield et al., 1994, 1995; Song et al., 1994), which also aims to achieve whole brain imaging in hundreds of milliseconds. When the gradient system has high amplitude and slew rate, EVI can be achieved by modifying the InI trajectory traversing a 3D k-space. In addition to the requirement on gradient performance, one concern of EVI is that the spatial resolution is also inhomogeneous as the result of different bandwidths in three orthogonal directions. Particularly, the narrowest bandwidth in EVI is around 100 Hz/pixel (Witzel et al., 2011), resulting in that the distortion and spatial resolution becomes rather poor in that specific direction.

Sampling rate

Currently InI uses the steady-state incoherent (SSI) pulse sequence (Haacke, 1999) to achieve 10 Hz sampling rate with whole-brain coverage. This sequence spoils the transverse magnetization by the end of each TR. In BOLD-contrast fMRI, the optimal echo time (TE) has been suggested to be the local $T2^*$ (Jezzard et al., 2001), which is about 30 ms at 3 T. Using a readout bandwidth of 2 kHz/pixel and an image matrix of 64×64, the readout takes only approximately 32 ms. Considering the time required for RF excitation, EPI pre-phasing, and RF/gradient spoiling, it is still possible to optimize the acquisition, such as using partial Fourier acquisition and reducing TE and thus the sensitivity to $T2^*$ changes, to further improve the sampling rate. However, for the optimal sensitivity, there are still tens of milliseconds between the RF excitation and the echo. This period of time prohibits a shorter TR.

However, it is possible to replace the SSI pulse sequence by the steady-state coherent (SSC) pulse sequence without compromising the optimal TE. Echo-shifting in the SSC pulse sequence allows TR > TE (Liu et al., 1993). This is particularly desirable in InI where TR needs to be as short as possible without modifying the optimal TE. In fact, the first InI study using echo-shifting for 2D fMRI showed that it is possible to achieve TR = 20 ms with TE = 43 ms at 1.5T (Lin et al., 2006). Recently, echo-shifting has been also implemented for volumetric InI to achieve TR = 25 ms with TE = 34 ms at 3T (Chang et al., 2011). Such sampling rate advancement comes at the price of reduced BOLD sensitivity (Liu et al., 1993).

Summary

InI is a novel fast BOLD sampling technique that is beginning to show promise in several applications. With advances in RF technology, pulse sequences, and image reconstruction algorithms, further improvements in its spatiotemporal resolution as well as the sensitivity to hemodynamic or even to neuronal responses may be possible. Accordingly, versatile applications of InI can be developed with trade-offs between resolution and sensitivity. These tools will hopefully help clinicians and neuroscientists in revealing the complex dynamics of the human brain.

Acknowledgments

The authors thank Drs. Jonathan R. Polimeni, Joseph B. Mandeville, and Wei-Tang Chang for essential technical support and inspiring discussions. This work was supported by National Institutes of Health Grants by R01DA14178, R01HD040712, R01NS037462, R01NS048279, P41RR14075, R01EB006847, R01EB000790, R01MH083744, R21DC010060, National Center for Research Resources, NSC 98-2320-B-002-004-MY3, NSC 100-2325-B-002-046 (National Science Council, Taiwan), NHRI-EX100-9715EC (National Health Research Institute, Taiwan), Academy of Finland (127624 and the FiDiPro program), Finnish Cultural Foundation, and Finnish Foundation for Technology Promotion.

References

Bammer, R., Keeling, S.L., Augustin, M., Pruessmann, K.P., Wolf, R., Stollberger, R., Hartung, H.P., Fazekas, F., 2001. Improved diffusion-weighted single-shot echo-planar imaging (EPI) in stroke using sensitivity encoding (SENSE). Magn. Reson. Med. 46, 548–554.
Bandettini, P.A., Jesmanowicz, A., Van Kylen, J., Birn, R.M., Hyde, J.S., 1998. Functional MRI of brain activation induced by scanner acoustic noise. Magn. Reson. Med. 39, 410–416.
Belliveau, J., Kennedy, D., McKinstry, R., Buchbinder, B., Weisskoff, R., Cohen, M., Vevea, J., Brady, T., Rosen, B., 1991. Functional mapping of the human visual cortex by magnetic resonance imaging. Science 254, 716–719.
Birn, R.M., Diamond, J.B., Smith, M.A., Bandettini, P.A., 2006. Separating respiratory-variation-related fluctuations from neuronal-activity-related fluctuations in fMRI. Neuroimage 31, 1536–1548.
Biswal, B., DeYoe, A.E., Hyde, J.S., 1996. Reduction of physiological fluctuations in fMRI using digital filters. Magn. Reson. Med. 35, 107–113.
Blum, M.J., Braun, M., Rosenfeld, D., 1987. Fast magnetic resonance imaging using spiral trajectories. Australas. Phys. Eng. Sci. Med. 10, 79–87.
Bodurka, J., Ledden, P.J., van Gelderen, P., Chu, R., de Zwart, J.A., Morris, D., Duyn, J.H., 2004. Scalable multichannel MRI data acquisition system. Magn. Reson. Med. 51, 165–171.
Bodurka, J., Ye, F., Petridou, N., Murphy, K., Bandettini, P.A., 2007. Mapping the MRI voxel volume in which thermal noise matches physiological noise—implications for fMRI. Neuroimage 34, 542–549.
Cabeza, R., McIntosh, A.R., Tulving, E., Nyberg, L., Grady, C.L., 1997. Age-related differences in effective neural connectivity during encoding and recall. Neuroreport 8, 3479–3483.
Chang, W.T., Nummenmaa, A., Hsieh, J.C., Lin, F.H., 2010. Spatially sparse source cluster modeling by compressive neuromagnetic tomography. Neuroimage 53, 146–160.
Chang, W.T., Witzel, T., Tsai, K., Kuo, W.J., Lin, F.H., 2011. Ultra-FastfMRI of human visual cortex using echo-shifted magnetic resonance inverse imaging. Proc Intl Soc Magn Reson Med, 631.
Chu, Y.H., Hung, Y.C., Lin, F.H., 2011. estimating causal interactions from fmrI time series using granger causality and transfer entropy. 17th annual meeting of the Organization on Human Brain Mapping, 751.
Dale, A., Buckner, R., 1997. Selective averaging of individual trials using fMRI. Hum. Brain Mapp. 5, 329–340.
de Zwart, J.A., Ledden, P.J., Kellman, P., van Gelderen, P., Duyn, J.H., 2002. Design of a SENSE-optimized high-sensitivity MRI receive coil for brain imaging. Magn. Reson. Med. 47, 1218–1227.
de Zwart, J.A., Ledden, P.J., van Gelderen, P., Bodurka, J., Chu, R., Duyn, J.H., 2004. Signal-to-noise ratio and parallel imaging performance of a 16-channel receive-only brain coil array at 3.0 Tesla. Magn. Reson. Med. 51, 22–26.
Deckers, R.H., van Gelderen, P., Ries, M., Barret, O., Duyn, J.H., Ikonomidou, V.N., Fukunaga, M., Glover, G.H., de Zwart, J.A., 2006. An adaptive filter for suppression of cardiac and respiratory noise in MRI time series data. Neuroimage 33, 1072–1081.
Deshpande, G., Sathian, K., Hu, X., 2010. Effect of hemodynamic variability on Granger causality analysis of fMRI. Neuroimage 52, 884–896.
Edmister, W.B., Talavage, T.M., Ledden, P.J., Weisskoff, R.M., 1999. Improved auditory cortex imaging using clustered volume acquisitions. Hum. Brain Mapp. 7, 89–97.
Feinberg, D.A., Moeller, S., Smith, S.M., Auerbach, E., Ramanna, S., Gunther, M., Glasser, M.F., Miller, K.L., Ugurbil, K., Yacoub, E., 2010. Multiplexed echo planar imaging for sub-second whole brain FMRI and fast diffusion imaging. PLoS One 5, e15710.
Friston, K.J., 2007. Statistical parametric mapping : the analysis of funtional brain images, 1st ed. Elsevier/Academic Press, Amsterdam ; Boston.
Friston, K.J., Frith, C.D., Liddle, P.F., Frackowiak, R.S., 1993. Functional connectivity: the principal-component analysis of large (PET) data sets. J. Cereb. Blood Flow Metab. 13, 5–14.
Friston, K.J., Buechel, C., Fink, G.R., Morris, J., Rolls, E., Dolan, R.J., 1997. Psychophysiological and modulatory interactions in neuroimaging. Neuroimage 6, 218–229.

Friston, K.J., Fletcher, P., Josephs, O., Holmes, A., Rugg, M.D., Turner, R., 1998. Event-related fMRI: characterizing differential responses. Neuroimage 7, 30–40.
Friston, K.J., Harrison, L., Penny, W., 2003. Dynamic causal modelling. Neuroimage 19, 1273–1302.
Glover, G.H., Li, T.Q., Ress, D., 2000. Image-based method for retrospective correction of physiological motion effects in fMRI: RETROICOR. Magn. Reson. Med. 44, 162–167.
Golay, X., Pruessmann, K.P., Weiger, M., Crelier, G.R., Folkers, P.J., Kollias, S.S., Boesiger, P., 2000. PRESTO-SENSE: an ultrafast whole-brain fMRI technique. Magn. Reson. Med. 43, 779–786.
Griswold, M.A., Jakob, P.M., Heidemann, R.M., Nittka, M., Jellus, V., Wang, J., Kiefer, B., Haase, A., 2002. Generalized autocalibrating partially parallel acquisitions (GRAPPA). Magn. Reson. Med. 47, 1202–1210.
Grotz, T., Zahneisen, B., Ella, A., Zaitsev, M., Hennig, J., 2009. Fast functional brain imaging using constrained reconstruction based on regularization using arbitrary projections. Magn. Reson. Med. 62, 394–405.
Haacke, E.M., 1999. Magnetic resonance imaging : physical principles and sequence design. J. Wiley & Sons, New York.
Hall, D.A., Haggard, M.P., Akeroyd, M.A., Palmer, A.R., Summerfield, A.Q., Elliott, M.R., Gurney, E.M., Bowtell, R.W., 1999. "Sparse" temporal sampling in auditory fMRI. Hum. Brain Mapp. 7, 213–223.
Hamalainen, M., Hari, R., Ilmoniemi, R., Knuutila, J., Lounasmaa, O., 1993. Magnetoencephalography-theory, instrumentation, and application to noninvasive studies of the working human brain. Rev. Mod. Phys. 65, 413–497.
Hennel, F., Girard, F., Loenneker, T., 1999. "Silent" MRI with soft gradient pulses. Magn. Reson. Med. 42, 6–10.
Hennig, J., 2005. Fast Imaging Horizons in Rapid MR Imaging. Intl Soc Magn Reson Med, Mansfield lecture.
Hennig, J., Zhong, K., Speck, O., 2007. MR-Encephalography: fast multi-channel monitoring of brain physiology with magnetic resonance. Neuroimage 34, 212–219.
Hu, X., Kim, S.G., 1994. Reduction of signal fluctuation in functional MRI using navigator echoes. Magn. Reson. Med. 31, 495–503.
Huettel, S., McCarthy, G., 2000. Evidence for a refractory period in the hemodynamic response to visual stimuli as measured by MRI. Neuroimage 11, 547–553.
Jezzard, P., Matthews, P.M., Smith, S.M., 2001. Functional MRI : an introduction to methods. Oxford University Press, Oxford ; New York.
Jones, R.A., Haraldseth, O., Muller, T.B., Rinck, P.A., Oksendal, A.N., 1993. K-space substitution: a novel dynamic imaging technique. Magn. Reson. Med. 29, 830–834.
Kasess, C., Moser, E., Windischberger, C., 2010. What temporal resolution is optimal for dynamic causal modeling? The 16th Annual Meeting of the Organization for Human Brain Mapping. The Organization for Human Brain Mapping, Barcelona, Spain.
Kayser, A.S., Sun, F.T., D'Esposito, M., 2009. A comparison of Granger causality and coherency in fMRI-based analysis of the motor system. Hum. Brain Mapp. 30, 3475–3494.
Kellman, P., McVeigh, E.R., 2001. Ghost artifact cancellation using phased array processing. Magn. Reson. Med. 46, 335–343.
Kim, S.G., Ogawa, S., 2002. Insights into new techniques for high resolution functional MRI. Curr. Opin. Neurobiol. 12, 607–615.
Kruger, G., Glover, G.H., 2001. Physiological noise in oxygenation-sensitive magnetic resonance imaging. Magn. Reson. Med. 46, 631–637.
Kwong, K.K., Belliveau, J.W., Chesler, D.A., Goldberg, I.E., Weisskoff, R.M., Poncelet, B.P., Kennedy, D.N., Hoppel, B.E., Cohen, M.S., Turner, R., Cheng, H., Brady, T.J., Rosen, B.R., 1992. Dynamic magnetic resonance imaging of human brain activity during primary sensory stimulation. Proc. Natl. Acad. Sci. U. S. A. 89, 5675–5679.
Larkman, D.J., Hajnal, J.V., Herlihy, A.H., Coutts, G.A., Young, I.R., Ehnholm, G., 2001. Use of multicoil arrays for separation of signal from multiple slices simultaneously excited. J. Magn. Reson. Imaging 13, 313–317.
Lee, H.-L., Zahneisen, B., Grotz, T., LeVan, P., Hennig, J., 2011. Resting-state networks at higher frequencies: a preliminary study. Proc Intl Soc Magn Reson Med, 1638.
LeVan, P., Zahneisen, B., Grotz, T., Hennig, J., 2011. A simultaneous EEG and high temporal resolution fMRI study of trial-by-trial fluctuations in visual evoked potentials. Proc Intl Soc Magn Reson Med, 108.
Lin, F.H., Kwong, K.K., Belliveau, J.W., Wald, L.L., 2004. Parallel imaging reconstruction using automatic regularization. Magn. Reson. Med. 559–567.
Lin, F.H., Huang, T.Y., Chen, N.K., Wang, F.N., Stufflebeam, S.M., Belliveau, J.W., Wald, L.L., Kwong, K.K., 2005. Functional MRI using regularized parallel imaging acquisition. Magn. Reson. Med. 343–353.
Lin, F., Wald, L., Ahlfors, S., Hamalainen, M., Kwong, K., Belliveau, J., 2006. Dynamic magnetic resonance inverse imaging of human brain function. Magn. Reson. Med. 56, 787–802.
Lin, F.H., Wang, F.N., Ahlfors, S.P., Hamalainen, M.S., Belliveau, J.W., 2007. Parallel MRI reconstruction using variance partitioning regularization. Magn. Reson. Med. 58, 735–744.
Lin, F.H., Witzel, T., Mandeville, J.B., Polimeni, J.R., Zeffiro, T.A., Greve, D.N., Wiggins, G., Wald, L.L., Belliveau, J.W., 2008a. Event-related single-shot volumetric functional magnetic resonance inverse imaging of visual processing. Neuroimage 42, 230–247.
Lin, F.H., Witzel, T., Zeffiro, T.A., Belliveau, J.W., 2008b. Linear constraint minimum variance beamformer functional magnetic resonance inverse imaging. Neuroimage 43, 297–311.
Lin, F.H., Agnew, J.A., Belliveau, J.W., Zeffiro, T.A., 2009. Functional and effective connectivity of visuomotor control systems demonstrated using generalized partial least squares and structural equation modeling. Hum. Brain Mapp. 30, 2232–2251.
Lin, F.H., Witzel, T., Chang, W.T., Wen-Kai Tsai, K., Wang, Y.H., Kuo, W.J., Belliveau, J.W., 2010a. K-space reconstruction of magnetic resonance inverse imaging (K-InI) of human visuomotor systems. Neuroimage 49, 3086–3098.
Lin, F.-H., Witzel, T., Raij, T., Ahveninen, J., Belliveau, J.W., 2010b. Relative timing of brain activations revealed by ultra-fast MR inverse imaging (InI). Proc. Intl. Soc. Mag. Reson. Med., Stockholm, Sweden, p. 268.
Lin, F.H., Ahveninen, J., Raij, T., Witzel, T., Chu, Y.H., Tsai, K., Kuo, W.J., Belliveau, J.W., 2011a. Increasing fMRI sampling rate improves granger causality estimates. 17th annual meeting of the Organization on Human Brain Mapping, 715.
Lin, F.H., Nummenmaa, A., Witzel, T., Polimeni, J.R., Zeffiro, T.A., Wang, F.N., Belliveau, J.W., in press. Physiological noise reduction using volumetric functional magnetic resonance inverse imaging. Hum. Brain Mapp. doi:10.1002/hbm.21403.
Liou, S.T., Witzel, T., Nummenmaa, A., Chang, W.T., Tsai, K.W., Kuo, W.J., Chung, H.W., Lin, F.H., 2011. Functional magnetic resonance inverse imaging of human visuomotor systems using eigenspace linearly constrained minimum amplitude (eLCMA) beamformer. Neuroimage 55, 87–100.
Liu, G., Sobering, G., Duyn, J., Moonen, C.T., 1993. A functional MRI technique combining principles of echo-shifting with a train of observations (PRESTO). Magn. Reson. Med. 30, 764–768.
Logothetis, N.K., Pauls, J., Augath, M., Trinath, T., Oeltermann, A., 2001. Neurophysiological investigation of the basis of the fMRI signal. Nature 412, 150–157.
Mansfield, P., 1977. Multi-planar image formation using NMR spin echos. J. Phys. C10, L55–L58.
Mansfield, P., Coxon, R., Glover, P., 1994. Echo-planar imaging of the brain at 3.0 T: first normal volunteer results. J. Comput. Assist. Tomogr. 18, 339–343.
Mansfield, P., Coxon, R., Hykin, J., 1995. Echo-volumar imaging (EVI) of the brain at 3.0 T: first normal volunteer and functional imaging results. J. Comput. Assist. Tomogr. 19, 847–852.
Mantini, D., Perrucci, M.G., Del Gratta, C., Romani, G.L., Corbetta, M., 2007. Electrophysiological signatures of resting state networks in the human brain. Proc. Natl. Acad. Sci. U. S. A. 104, 13170–13175.
Matsuura, K., Okabe, U., 1995. Selective minimum-norm solution of the biomagnetic inverse problem. IEEE Trans. Biomed. Eng. 42, 608–615.
McDougall, M.P., Wright, S.M., 2005. 64-channel array coil for single echo acquisition magnetic resonance imaging. Magn. Reson. Med. 54, 386–392.
McGibney, G., Smith, M.R., Nichols, S.T., Crawley, A., 1993. Quantitative evaluation of several partial Fourier reconstruction algorithms used in MRI. Magn. Reson. Med. 30, 51–59.
McIntosh, A.R., Gonzalez-Lima, F., 1994. Structural equation modeling and its application to network analysis in functional brain imaging. Hum. Brain Mapp. 2, 2–22.
Menon, R.S., Luknowsky, D.C., Gati, J.S., 1998. Mental chronometry using latency-resolved functional MRI. Proc. Natl. Acad. Sci. U. S. A. 95, 10902–10907.
Ogawa, S., Lee, T.M., Kay, A.R., Tank, D.W., 1990. Brain magnetic resonance imaging with contrast dependent on blood oxygenation. Proc. Natl. Acad. Sci. U. S. A. 87, 9868–9872.
Ogawa, S., Lee, T.M., Stepnoski, R., Chen, W., Zhu, X.H., Ugurbil, K., 2000. An approach to probe some neural systems interaction by functional MRI at neural time scale down to milliseconds. Proc. Natl. Acad. Sci. U. S. A. 97, 11026–11031.
Ohliger, M.A., Grant, A.K., Sodickson, D.K., 2003. Ultimate intrinsic signal-to-noise ratio for parallel MRI: electromagnetic field considerations. Magn. Reson. Med. 50, 1018–1030.
Panych, L.P., Jakab, P.D., Jolesz, F.A., 1993. Implementation of wavelet-encoded MR imaging. J. Magn. Reson. Imaging 3, 649–655.
Poser, B.A., Norris, D.G., 2009. Investigating the benefits of multi-echo EPI for fMRI at 7 T. Neuroimage 45, 1162–1172.
Posse, S., Wiese, S., Gembris, D., Mathiak, K., Kessler, C., Grosse-Ruyken, M.L., Elghahwagi, B., Richards, T., Dager, S.R., Kiselev, V.G., 1999. Enhancement of BOLD-contrast sensitivity by single-shot multi-echo functional MR imaging. Magn. Reson. Med. 42, 87–97.
Preibisch, C., Pilatus, U., Bunke, J., Hoogenraad, F., Zanella, F., Lanfermann, H., 2003. Functional MRI using sensitivity-encoded echo planar imaging (SENSE-EPI). Neuroimage 19, 412–421.
Pruessmann, K.P., Weiger, M., Scheidegger, M.B., Boesiger, P., 1999. SENSE: sensitivity encoding for fast MRI. Magn. Reson. Med. 42, 952–962.
Raichle, M.E., MacLeod, A.M., Snyder, A.Z., Powers, W.J., Gusnard, D.A., Shulman, G.L., 2001. A default mode of brain function. Proc. Natl. Acad. Sci. U. S. A. 98, 676–682.
Raij, T., Ahveninen, J., Lin, F.H., Witzel, T., Jaaskelainen, I.P., Letham, B., Israeli, E., Sahyoun, C., Vasios, C., Stufflebeam, S., Hamalainen, M., Belliveau, J.W., 2010. Onset timing of cross-sensory activations and multisensory interactions in auditory and visual sensory cortices. Eur. J. Neurosci. 31, 1772–1782.
Richter, W., Somorjai, R., Summers, R., Jarmasz, M., Menon, R.S., Gati, J.S., Georgopoulos, A.P., Tegeler, C., Ugurbil, K., Kim, S.G., 2000. Motor area activity during mental rotation studied by time-resolved single-trial fMRI. J. Cogn. Neurosci. 12, 310–320.
Roebroeck, A., Formisano, E., Goebel, R., 2005. Mapping directed influence over the brain using Granger causality and fMRI. Neuroimage 25, 230–242.
Rosen, B.R., Buckner, R.L., Dale, A.M., 1998. Event-related functional MRI: past, present, and future. Proc. Natl. Acad. Sci. U. S. A. 95, 773–780.
Schmidt, C.F., Degonda, N., Luechinger, R., Henke, K., Boesiger, P., 2005. Sensitivity-encoded (SENSE) echo planar fMRI at 3T in the medial temporal lobe. Neuroimage 25, 625–641.
Schmitt, F., Stehling, M.K., Turner, R., Bandettini, P.A., 1998. Echo-planar imaging : theory, technique, and application. Springer, Berlin ; New York.
Schwarzbauer, C., Davis, M.H., Rodd, J.M., Johnsrude, I., 2006. Interleaved silent steady state (ISSS) imaging: a new sparse imaging method applied to auditory fMRI. Neuroimage 29, 774–782.
Setsompop, K., Gagoski, B.A., Polimeni, J.R., Witzel, T., Wedeen, V.J., Wald, L.L., 2012. Blipped-controlled aliasing in parallel imaging for simultaneous multislice echo planer imaging with reduced g-factor penalty. Magn. Reson. Med. 67, 1210–1224.
Singer, W., 1999. Neuronal synchrony: a versatile code for the definition of relations? Neuron 24, 49–65 111–125.

Smith, S.M., Miller, K.L., Salimi-Khorshidi, G., Webster, M., Beckmann, C.F., Nichols, T.E., Ramsey, J.D., Woolrich, M.W., 2011. Network modelling methods for FMRI. Neuroimage 54, 875–891.
Sodickson, D.K., Manning, W.J., 1997. Simultaneous acquisition of spatial harmonics (SMASH): fast imaging with radiofrequency coil arrays. Magn. Reson. Med. 38, 591–603.
Sodickson, D.K., McKenzie, C.A., 2001. A generalized approach to parallel magnetic resonance imaging. Med. Phys. 28, 1629–1643.
Song, A.W., Wong, E.C., Hyde, J.S., 1994. Echo-volume imaging. Magn. Reson. Med. 32, 668–671.
Talavage, T.M., Edmister, W.B., Ledden, P.J., Weisskoff, R.M., 1999. Quantitative assessment of auditory cortex responses induced by imager acoustic noise. Hum. Brain Mapp. 7, 79–88.
Tarantola, A., 2005. Inverse problem theory and methods for model parameter estimation. Society for Industrial and Applied Mathematics, Philadelphia, PA.
Tsai, K., Numenmaa, A., Witzel, T., Chang, W.T., Kuo, W.J., Lin, F.H., 2011. Dynamic magnetic resonance multi-projection InverseImaging (Mini) with isotropic spatial resolution. Proc Intl Soc Magn Reson Med, 632.
Tsao, J., Behnia, B., Webb, A.G., 2001. Unifying linear prior-information-driven methods for accelerated image acquisition. Magn. Reson. Med. 46, 652–660.
Uutela, K., Hamalainen, M., Somersalo, E., 1999. Visualization of magnetoencephalographic data using minimum current estimates. Neuroimage 10, 173–180.
van Vaals, J.J., Brummer, M.E., Dixon, W.T., Tuithof, H.H., Engels, H., Nelson, R.C., Gerety, B.M., Chezmar, J.L., den Boer, J.A., 1993. "Keyhole" method for accelerating imaging of contrast agent uptake. J. Magn. Reson. Imaging 3, 671–675.
Weaver, J.B., Xu, Y., Healy, D.M., Driscoll, J.R., 1992. Wavelet-encoded MR imaging. Magn. Reson. Med. 24, 275–287.
Weiger, M., Pruessmann, K.P., Osterbauer, R., Bornert, P., Boesiger, P., Jezzard, P., 2002. Sensitivity-encoded single-shot spiral imaging for reduced susceptibility artifacts in BOLD fMRI. Magn. Reson. Med. 48, 860–866.
Wiesinger, F., Boesiger, P., Pruessmann, K.P., 2004. Electrodynamics and ultimate SNR in parallel MR imaging. Magn. Reson. Med. 52, 376–390.
Wiggins, G.C., Potthast, A., Triantafyllou, C., Lin, F.-H., Benner, T., Wiggins, C.J., Wald, L.L., 2005a. A 96-channel MRI system with 23- and 90-channel phase array head coils at 1.5 Tesla. International Society for Magnetic Resonance in Medicine Thirteenth Scientific Meeting and Exhibition. International Society for Magnetic Resonance in Medicine, Miami, Florida, USA, p. 671.
Wiggins, G.C., Triantafyllou, C., Potthast, A., Reykowski, A., Nittka, M., Wald, L.L., 2005b. A 32 Channel Receive-only Phased Array Head Coil for 3T with Novel Geodesic Tiling Geometry. International Society for Magnetic Resonance in Medicine Thirteenth Scientific Meeting and Exhibition. International Society for Magnetic Resonance in Medicine, Miami, Florida, USA, p. 671.
Wiggins, G.C., Polimeni, J.R., Potthast, A., Schmitt, M., Alagappan, V., Wald, L.L., 2009. 96-Channel receive-only head coil for 3 Tesla: design optimization and evaluation. Magn. Reson. Med. 62, 754–762.
Witzel, T., Polimeni, J.R., Lin, F.H., Numenmaa, A., Wald, L.L., 2011. Single-shot whole brain echo volume imaging for temporally resolved physiological signals in fMRI. Proc Intl Soc Magn Reson Med, 633.
Xiong, J., Fox, P.T., Gao, J.H., 2003. Directly mapping magnetic field effects of neuronal activity by magnetic resonance imaging. Hum. Brain Mapp. 20, 41–49.
Zahneisen, B., Grotz, T., Lee, K.J., Ohlendorf, S., Reisert, M., Zaitsev, M., Hennig, J., 2011a. Three-dimensional MR-encephalography: fast volumetric brain imaging using rosette trajectories. Magn. Reson. Med. 65, 1260–1268.
Zahneisen, B., Grotz, T., Zaitsev, M., Hennig, J., 2011b. Ultra fast volumetric functional imaging using single shot concentric shells trajectories. Proc Intl Soc Magn Reson Med, 4360.
Zhang, N., Zhu, X.H., Chen, W., 2005. Influence of gradient acoustic noise on fMRI response in the human visual cortex. Magn. Reson. Med. 54, 258–263.
Zientara, G.P., Panych, L.P., Jolesz, F.A., 1994. Dynamically adaptive MRI with encoding by singular value decomposition. Magn. Reson. Med. 32, 268–274.